

Spinal Codes Optimization: Error Probability Analysis and Transmission Scheme Design

Aimin Li, Shaohua Wu, Jian Jiao, Ning Zhang, and Qinyu Zhang

Abstract—Spinal codes are known to be capacity achieving over both the additive white Gaussian noise (AWGN) channel and the binary symmetric channel (BSC). Over wireless channels, Spinal encoding can also be regarded as an adaptive-coded-modulation (ACM) technique due to its rateless property, which fits it with mobile communications. Due to lack of tight analysis on error probability of Spinal codes, optimization of transmission scheme using Spinal codes has not been fully explored. In this work, we firstly derive new tight upper bounds of the frame error rate (FER) of Spinal codes for both the AWGN channel and the BSC in the finite block-length (FBL) regime. Based on the derived upper bounds, we then design the optimal transmission scheme. Specifically, we formulate a rate maximization problem as a nonlinear integer programming problem, and solve it by an iterative algorithm for its dual problem. As the optimal solution exhibits an incremental-tail-transmission pattern, we propose an improved transmission scheme for Spinal codes. Moreover, we develop a bubble decoding with memory (BD-M) algorithm to reduce the decoding time complexity without loss of rate performance. The improved transmission scheme at the transmitter and the BD-M algorithm at the receiver jointly constitute an "encoding-decoding" system of Spinal codes. Simulation results demonstrate that it can improve both the rate performance and the decoding throughput of Spinal codes.

Index Terms—Spinal codes, FER analysis, rate maximization, transmission scheme, low complexity decoding.

I. INTRODUCTION

AS a new type of capacity-achieving codes, Spinal codes have been proved to be capacity-achieving over both the additive white Gaussian noise (AWGN) channel and the binary symmetric channel (BSC) [3][4]. Different from other channel codes, such as Turbo/LDPC codes [5][6], digital fountain codes [7][8] and Strider codes [9], Spinal codes combine a hash function with a random number generator (RNG) to generate pseudo-random coding symbols for transmission. The pairwise independent feature of the hash function ensures that the coding symbols are approximately independent with each other. The use of RNG inherits from the idea of Shannon random coding, which gives the coding symbols pseudo-random characteristics. The combination of the hash function and the RNG ensures that the coding symbols are approximately independent and identically distributed (i.i.d), which leads to an excellent rate performance of Spinal codes.

As a type of rateless codes, Spinal codes do not need to frequently estimate the channel state to adjust the code rate and modulation mode. Instead, it keeps generating and transmitting the pseudo-random coding symbols until the transmitted symbols are sufficient for the decoder to decode successfully and an acknowledgment (ACK) is fed back to the transmitter to interrupt the symbol transmission. By this means, Spinal codes is able to automatically select the most appropriate code rate to ensure the reliable transmission when the channel state information is unknown. The rateless property of Spinal fits Spinal codes with wireless channel application scenarios, such as vehicular communications and satellite communications.

Combining the above two points, the capacity-achieving characteristic and the rateless feature collectively enable Spinal codes to possess enormously practical value. However, high-frequency use of hash function together with multiple tentative decoding at the decoder can result in extremely high decoding time complexity. In the literature, many decoding algorithms have been proposed to reduce the decoding time complexity of Spinal codes. In [10], the proposed forward stack decoding (FSD) can decrease the decoding time complexity significantly without sacrificing the rate performance. In [11], the sliding window decoding (SFD) algorithm is proposed, which outperforms FSD in terms of much lower decoding time complexity without degrading rate performance much. In [12], the block dynamic decoding (BDD) algorithm is proposed, which introduces dynamic parameters in the process of decoding to reduce both time complexity and FER of Spinal codes. The works on designing high-efficiency decoding algorithms have made remarkable contributions for Spinal codes on its way from theory to practice. However, the existing researches mainly focus on the structure of the decoding tree itself. Different pruning strategies are designed to reduce the calculation required to reconstruct the decoding tree; while the decoding algorithm which explores jointly the decoder's decoding state at the receiver as well as the transmission scheme at the transmitter are seldom investigated.

As for the transmission scheme design, puncturing on the coded symbols is commonly adopted as an efficient method to improve rate performance. In [13], coding schemes that can be punctured to adapt to time-varying channels are known as rate-compatible codes. As the redundant symbols are punctured, the code rate generally increases. As a result, puncturing technology has drawn extensive interests in the literature, such as punctured LDPC codes in [14] and punctured Turbo codes in [15]. For Spinal codes, the uniform puncturing based transmission scheme is proposed in [16], where the whole pass is divided into many sub-passes and the transmitter only

Part of the work was presented at ICC' 2019 [1] and VTC2020-Spring [2].

A. Li, S. Wu, J. Jiao and Q. Zhang are with the Department of Electronic Engineering, Harbin Institute of Technology (Shenzhen), Guangdong, China (e-mail: hitliaimin@163.com; hitwush@hit.edu.cn; jiaojian@hit.edu.cn; zqy@hit.edu.cn).

N. Zhang are with the Department of Electrical and Computer Engineering University of Windsor, Windsor, Canada (e-mail: ning.zhang@uwindsor.ca).

transmits a single symbol in a sub-pass to obtain a finer-grained rate set. In [17], the uniform puncturing is improved and adopted in S-Spinal codes to achieve finer granularity for compression purposes. As the uniform puncturing based transmission scheme is only a general puncturing method for rateless codes, transmission scheme that exploits the unique properties of Spinal codes are expected to be designed [1].

Error probability analysis of Spinal codes in FBL domain is a fundamental prerequisite for mathematically formulating the transmission scheme design problem. In [4], the capacity achievability of Spinal codes is proved in theory, wherein the error probability analysis simply considers Spinal codes as an ideal random codes with pairwise independent property and introduces an unusual application of a variant of Gallager's result [18]. The analysis somehow reflects the asymptotic performance of Spinal code only if the block length is infinite. To analyze the error probability of Spinal codes under the regime of FBL, the serial coding structure of Spinal codes needs to be taken into account. In [19], the serial coding structure of Spinal codes is considered, and the general upper bounds on pairwise independent random codes over the AWGN channel and the BSC are introduced as kernels to analyze the upper bounds of error probability for different priorities of serial unequal error protection (UEP) Spinal codes. Nevertheless, in the derivation process, instead of taking the featured decoding process of Spinal codes into account, the authors take the general upper bounds of pairwise independent random code as cores to analyze the error probability of Spinal codes, which results in over-evaluated upper bounds of FER. In short, more accurate and tighter upper bounds of FER of Spinal codes that fully consider the featured coding and decoding process is still to be proposed in the literature.

In this paper, we aim to design an optimized transmission scheme for Spinal codes. Considering the aforementioned factors, we begin with re-analyzing the FER of Spinal codes over both the BSC and the AWGN channel under the regime of FBL. Our analysis fully considers the whole coding and decoding process of Spinal codes, including the segmented and serial coding structure of Spinal codes, the combination of hash function and RNG, and the ML decoding process of Spinal codes. Then, based on the derived bounds, we formulate a rate maximization problem as a nonlinear integer programming problem. To solve the problem, we consider its dual problem and devise an iterative algorithm. The optimal solution turns out to an incremental-tail-transmission pattern, based on which we propose the improved transmission scheme, which achieves a much better rate performance than the original uniform puncturing based transmission scheme. Furthermore, to address the high time complexity issue at the receiver, we design a low-time-complexity decoding algorithm, named bubble decoding with memory (BD-M), which matches well with the proposed transmission scheme. The improved transmission scheme at the transmitter together with the matching decoding algorithm at the decoder constitute an optimized transmission system for Spinal codes, which can not only improve the rate performance of Spinal codes but also reduces the decoding time complexity.

The main contributions of this work can be summarized as follows:

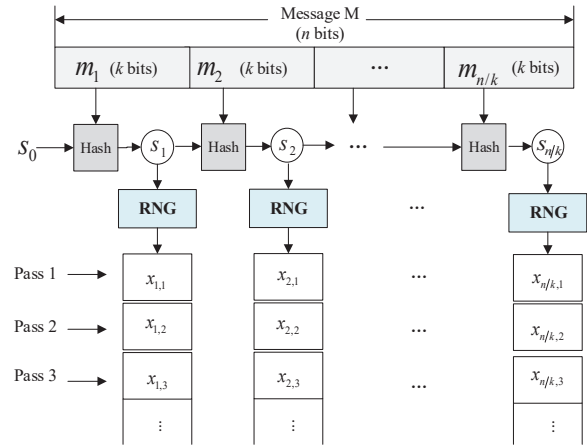


Fig. 1. The encoding process of Spinal codes.

- We derive new non-asymptotically upper bounds of the FER of Spinal codes over both the AWGN channel and the BSC.
- We propose an optimized transmission scheme for Spinal codes by formulating and solving the rate maximization problem based on the derived FER upper bounds, which further enhances the rate performance of Spinal codes.
- We propose a low-complexity decoding algorithm named BD-M, which matches the proposed transmission scheme well and reduces the decoding time complexity without loss of rate performance.

The rest of this paper is organized as follows. Section II introduces the preliminaries of Spinal codes. In Section III, the new FER upper bounds of Spinal codes are derived. The details of the transmission scheme design are presented in Section IV. In Section V, the low-complexity decoding algorithm and its complexity analysis are presented. In Section VI, simulation results are provided, followed by conclusions in Section VII.

II. PRELIMINARIES

A. Encoding Process of Spinal Codes

The hash function is the core of Spinal codes, which is combined with the RNG to continuously generate approximately i.i.d pseudo-random symbols. As shown in Fig. 1, the encoding process of Spinal codes can be accomplished in 4 steps:

- 1) An n -bit message M is divided into some k -bit segments, denoted by m_i , where $i = 1, 2, \dots, n/k$.
- 2) The hash function is invoked iteratively to map m_i to a v -bit state value s_i :

$$s_i = h(s_{i-1}, m_i), s_0 = 0^v, \quad (1)$$

where s_0 is the initial value known by both the encoder and the decoder.

- 3) The v -bit state value s_i serves as a seed of the RNG to generate pseudo-random c -bit symbols denoted by $x_{i,j}$:

$$\text{RNG} : s_i \times \mathbb{N} \rightarrow x_{i,j}, \quad (2)$$

where $x_{i,j} \in \{0,1\}^c$, $s_i \in \{0,1\}^v$.

- 4) The encoder maps the c -bit symbols to a channel input set to fit the channel characteristics:

$$f : x_{i,j} \rightarrow \Omega, \quad (3)$$

where f is a constellation mapping function, Ω denotes the channel input set. For the BSC, the constellation mapping is trivial with $c = 1$, and the sender transmits $x_{i,j}$ directly.

The transmitter will continuously transmit the coding symbols pass-by-pass unless the transmitted symbols are sufficient for successful decoding and an ACK is sent to the transmitter.

As a kind of rateless code, Spinal codes possess excellent rate performance due to the combination of the hash function and the RNG. Specifically, the pairwise independent feature of the hash function ensures the approximate independence of Spinal codes based coding symbols, and the RNG makes the coding symbols pseudo-random.

B. Decoding Process of Spinal Codes

For Spinal codes, the optimal decoding algorithm is the maximum likelihood (ML) decoding. In the ML decoding, the decoder adopts the shared knowledge of the same hash function, the same initial state value s_0 and the same RNG to replay the coding process over the set of received symbols. In other words, the decoder aims to find the best matching sequence $\hat{M} \in \{0,1\}^n$ whose encoded vector $\mathbf{x}(\hat{M})$ is closest to the received vector \mathbf{y} in Euclidean distance. The ML rule can be expressed as:

$$\begin{aligned} \hat{M} &= \arg \min_{M' \in (0,1)^n} \|\mathbf{y} - \mathbf{x}(M')\| \\ &= \arg \min_{M' \in (0,1)^n} \sum_{i=1}^{n/k} \sum_{j=1}^{l_i} \|y_{i,j} - x_{i,j}(M')\|, \end{aligned} \quad (4)$$

where \hat{M} is the decoding result, M' represents the candidate sequence and l_i is the number of symbols generated from the i^{th} spine value of the n -bit message M .

However, traversing all candidate sequences M' results in an exponential increase in complexity. The serial coding structure of Spinal codes determines that Spinal codes are a type of tree code. As a result, the bubble decoding proposed in [16] can be applied to decrease the decoding complexity. Instead of searching the entire decoding tree, the bubble decoder calculates the *Cost* for the nodes at each layer and sort them to retain only B best candidate nodes with the lowest cost at each layer. The reserved nodes then expand $B \cdot 2^k$ child nodes related to the B nodes at the next layer. It repeats until the bubble decoder ends up with a list of B messages at the last layer, from which the best one is selected as the decoding output. The cost at each layer can be calculated as:

$$Cost = \sum_{i=1}^{layer} \sum_{j=1}^{l_i} \|y_{i,j} - x_{i,j}(M')\|, \quad (5)$$

where *layer* denotes the currently expanded number of layers.

C. Rateless Transmission scheme

As a kind of rateless code, Spinal codes continuously transmit the coding symbols unless an ACK is sent to interrupt the transmission. The original transmission scheme for Spinal codes is a pass-by-pass transmission scheme. For example, the transmitter firstly transmits a pass of encoded symbols $\mathbf{X}_{PASS1} = [x_{1,1}, x_{2,1}, \dots, x_{n/k,1}]$. When the receiver receives the symbols, it will conduct tentative decoding to observe whether the received symbols are enough to recover the message. Meanwhile, the transmitter will continuously send encoded symbols pass by pass until the number of received symbols is enough for successful decoding and an ACK is sent to end the transmission.

For the pass-by-pass transmission scheme, the rate granularity is too coarse, and there may be redundant transmitted symbols in the last pass transmission. To refine the rate granularity, the uniform puncturing based transmission scheme is generally designed. In [16], the authors propose a uniform puncturing based transmission scheme for Spinal codes, which uniformly divides the integral transmission pass into several sub-passes to obtain a finer-grained rate set.

Taking $n/k = 8$, i.e., an 8-segment coding structure as an example, Fig. 2 shows the uniform puncturing based transmission scheme for Spinal codes. Each pass is equally divided into eight sub-passes, which is illustrated by the eight rows in the figure. We set $\vec{g} = [g_1, g_2, \dots, g_8]$ to denote the transmission order of the symbols. The elements in \vec{g} are indexes of sub-passes. According to \vec{g} , the sender transmits the g_i^{th} symbol in order, where $i \in \{1, 2, \dots, n/k\}$. The sender transmits the symbols sub-pass by sub-pass until an ACK is received.

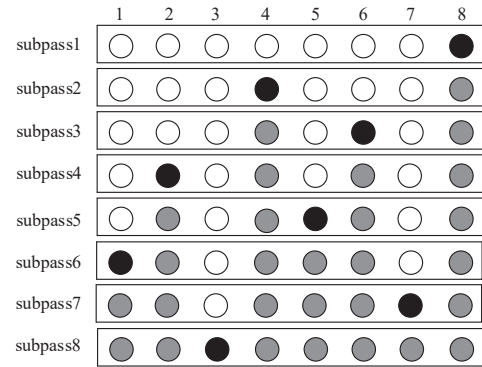


Fig. 2. The uniform puncturing with $\vec{g} = [8, 4, 6, 2, 5, 1, 7, 3]$. In each sub-pass, the sender transmits the symbols marked by dark circles while those shaded circles represent symbols that have already been sent in previous sub-passes.

Although the uniform puncturing based transmission scheme indeed improves the rate performance, there are still some shortcomings. First of all, the property of forwardly increasing redundancy of Spinal codes is neglected in the uniform puncturing based transmission scheme. Secondly, the refinement of the code rate increases the decoding attempts at the receiver, and thus reduces the decoding throughput of Spinal codes.

D. Error Probability Analysis by Applying General Bounds of Random Codes (Previous works)

In [20], the authors prove the capacity achievability of Spinal codes, but referring to the error probability of Spinal codes, it simply regards Spinal codes as an ideal random code with ideal pairwise independence property and introduces an unusual application of a variant of Gallager's famous result [18]. To a certain extent, the analysis can be used to describe the asymptotic performance of Spinal codes with infinite block length, however, since it neglects the serial coding structure of Spinal codes, the analysis is not exact under the regime of FBL.

In [19], the authors take the serial coding structure of Spinal codes into account and introduce the general upper bounds of random codes over the AWGN channel and the BSC, the variant of Gallager's bound [18] and the random coding union bound (RCU) [21] as kernels to analyze the upper bound of error probability of Spinal codes. For comparison purpose, we briefly summarize the results in [19] as follows.

Theorem 1. (The FER upper bound of Spinal codes over AWGN in [19]) Consider Spinal codes with message length n and segmentation parameter k transmitted over an AWGN channel with noise variance σ^2 . Let L be the number of passes the receiver received. Then, the average error probability under ML decoding can be upper bounded by

$$P_e \leq 1 - \prod_{i=1}^{n/k} (1 - \epsilon_i^{upper}(T_i, U_i)), \quad (6)$$

with

$$\epsilon_i^{upper}(T_i, U_i) = 2^{-T_i(E_0(Q) - \frac{\log T_i}{U_i})}, \quad (7)$$

where $T_i = L(n/k - i + 1)$, $U_i = 2^{k(n/k - i + 1)}$, Q denotes the distribution of the channel input and

$$E_0(Q) = -\log_2 \left\{ \frac{1}{\sqrt{2\pi\sigma^2}} \times \int_{\mathbb{R}} \left(\sum_{x \in \Omega} Q(x) \cdot \exp\left(-\frac{(y-x)^2}{4\sigma^2}\right) \right)^2 dy \right\}. \quad (8)$$

The proof of Theorem 1 applies a variant of Gallager's bound, which is $P_e \leq 2^{-T(E_0(Q) - R)}$, where T denotes the block length and $R = n/T$ represents the rate. We refer the readers to [19] for more details of the proof.

Theorem 2. (The FER upper bound of Spinal codes over BSC in [19]) Consider Spinal codes with message length n and segmentation parameter k transmitted over a BSC with crossover probability f . Let L be the number of passes at the receiver. Then, the average error probability under ML decoding can be upper bounded by

$$P_e \leq 1 - \prod_{i=1}^{n/k} (1 - \epsilon_i^{upper}(T_i, U_i)), \quad (9)$$

with

$$\epsilon_i^{upper}(T_i, U_i) = \sum_{t=0}^{T_i} \left\{ \binom{T_i}{t} f^t (1-f)^{T_i-t} \times \min \left[1, (U_i - 1) \sum_{k=0}^t \binom{T_i}{k} 2^{-T_i} \right] \right\}, \quad (10)$$

where $T_i = L(n/k - i + 1)$, $U_i = 2^{k(n/k - i + 1)}$.

The proof of Theorem 2 is similar to the proof of Theorem 1, the only difference is that the proof of Theorem 1 adopts a variant of Gallager's bound, while the proof of Theorem 2 applies the RCU bound.

Remark 1. Both the FER upper bounds analyses in [20] and [19] are based on the assumptions that Spinal codes have ideal pairwise independence, the RNG can provide completely random characteristics, and the ACK will be sent only if the decoding result is exactly the same as the transmitted message sequence. In this paper, our analysis will be also carried out under the above three basic assumptions.

III. NEW FER UPPER BOUNDS OF SPINAL CODES

In this section, we re-analyze the error probability of Spinal codes, by fully taking the coding structure and the decoding process in the derivations into account. Through analysis, new tighter upper bounds of Spinal codes over both the AWGN channel and the BSC are obtained. These upper bounds will serve as the theoretic basis for the transmission scheme design in Section IV.

A. FER Upper Bound analysis of Spinal Codes over AWGN

As reviewed in Section II.D, the general upper bounds of pairwise independent random codes are used to analyze the FER of Spinal codes over the BSC and the AWGN channel. However, the analytical process does not fully consider the concrete coding and decoding process of Spinal codes itself. In this subsection, we aim to derive a tighter FER approximation of Spinal codes over AWGN, which is customized for Spinal codes and more closely fits the simulated FER of Spinal codes. In our derivation, the whole coding and decoding process of Spinal codes have been fully considered, including the segmented and serial coding structure of Spinal codes, the combination of hash function and RNG, and the ML decoding process of Spinal codes.

Theorem 3. (New FER upper bound of Spinal codes over AWGN) Consider Spinal codes with message length n , segmentation parameter k and modulation parameter c transmitted over an AWGN channel with noise variance σ^2 , then the FER under ML decoding can be upper bounded by

$$P_e \leq 1 - \prod_{i=1}^{n/k} (1 - \epsilon_i), \quad (11)$$

with

$$\epsilon_i = \min \{1, (2^k - 1) 2^{n-ik} \cdot \min(1, R_i)\}, \quad (12)$$

where

$$R_i = \frac{1}{\Gamma\left(1 + \sum_{j=i}^{n/k} l_j / 2\right)} \left(\frac{\pi (1+\varepsilon) \sigma^2 \sum_{j=i}^{n/k} l_j}{2^{2c}} \right)^{\sum_{j=i}^{n/k} l_j / 2}, \quad (13)$$

where $\Gamma(\cdot)$ denotes the Gamma function, and l_j is the number of symbols generated from the j^{th} spine value of the n -bit message sequence.

Proof. Suppose that message $M = (m_1, m_2, \dots, m_{n/k})$. Let $x_{i,j}(M)$ denote the j^{th} coding symbols generated from the i^{th} spine value s_i of the n -bit message M , $y_{i,j}$ denote the corresponding symbols received by the receiver, and $n_{i,j}$ represent the corresponding white Gaussian noise. It is easy to obtain that

$$y_{i,j} = x_{i,j}(M) + n_{i,j}. \quad (14)$$

For Spinal codes over AWGN channel, the ML decoding algorithm is straightforward, with

$$\begin{aligned} \hat{M} &= \arg \min_{M' \in (0,1)^n} \|\mathbf{y} - \mathbf{x}(M')\| \\ &= \arg \min_{M' \in (0,1)^n} \sum_{i=1}^{n/k} \sum_{j=1}^{l_i} \|y_{i,j} - x_{i,j}(M')\|, \end{aligned} \quad (15)$$

where M' denotes the candidate sequence and l_i is the number of symbols generated from the i^{th} spine value of the n -bit message M .

Similarly, we classify the candidate sequence set into two subsets: M'_{correct} and M'_{wrong} .

(1) Firstly, we analyze the cost of the candidate sequence in M'_{correct} , which is denoted by $D(m'_{\text{correct}})$.

$$\begin{aligned} D(m'_{\text{correct}}) &= \sum_{i=1}^{n/k} \sum_{j=1}^{l_i} (y_{i,j} - x_{i,j}(m'_{\text{correct}}))^2 \\ &= \sum_{i=1}^{n/k} \sum_{j=1}^{l_i} n_{i,j}^2. \end{aligned} \quad (16)$$

Because $\mathbb{E}(n_{i,j}^2) = \sigma^2$, by applying the chernoff bound, we possess probability of $1 - O\left(\exp\left(-\Theta\left(\varepsilon^2 \sum_{i=1}^{n/k} l_i\right)\right)\right)$ to assure that

$$D(m'_{\text{correct}}) \leq (1+\varepsilon) \sigma^2 \sum_{i=1}^{n/k} l_i. \quad (17)$$

(2) Secondly, we analyze the cost of the candidate sequence in M'_{wrong} , which is denoted by $D(m'_{\text{wrong}})$. The FER of Spinal codes is

$$P_e = \mathbb{P}(\exists m'_{\text{wrong}} : D(m'_{\text{wrong}}) \leq D(m'_{\text{correct}})). \quad (18)$$

Let $M'_{\text{wrong}} = [m'_1, m'_2, \dots, m'_{n/k}]$ denote the set of wrong sequences with $m'_1 \neq m_1$ and let E_i represent the event that there exists an error in the i^{th} segment. By applying Eq.(17)

and the union bound of probability, the probability of E_1 can be bounded as

$$\begin{aligned} \mathbb{P}(E_1) &\leq \sum_{m'_{\text{wrong}}} \mathbb{P}(D(m'_{\text{wrong}}) \leq D(m'_{\text{correct}})) \\ &\leq \sum_{m'_{\text{wrong}}} \mathbb{P}\left(D(m'_{\text{wrong}}) \leq (1+\varepsilon) \sigma^2 \sum_{j=1}^{n/k} l_j\right). \end{aligned} \quad (19)$$

Due to Spinal codes' coding structure which combines hash function and RNG, all the coded symbols of m'_{correct} and m'_{wrong} are mapped independently and randomly. Now for the uniform constellation, it is easy to verify that the coded symbols $x_{i,j}(m'_{\text{correct}})$ and $x_{i,j}(m'_{\text{wrong}})$ are independent of each other with uniform distribution. Therefore, we approximate the probability in (19) as follows.

$$\begin{aligned} &\mathbb{P}\left(D(m'_{\text{wrong}}) \leq (1+\varepsilon) \sigma^2 \sum_{i=1}^{n/k} l_i\right) \approx \\ &\frac{\text{Volume of a ball with radius } r = \sqrt{(1+\varepsilon) \sigma^2 \sum_{i=1}^{n/k} l_i}}{\text{Volume of a cube } [0, 2^c - 1]_{i=1}^{n/k} l_i} \\ &= \frac{1}{\Gamma\left(1 + \sum_{i=1}^{n/k} l_i / 2\right)} \left(\frac{\pi (1+\varepsilon) \sigma^2 \sum_{i=1}^{n/k} l_i}{2^{2c}} \right)^{\sum_{i=1}^{n/k} l_i / 2}, \end{aligned} \quad (20)$$

where the dimensions of the ball and the cube are both $\sum_{i=1}^{n/k} l_i$. Since the volume of the ball in (20) might be larger than the volume of the cube when σ^2 is large, the function $\min(1, \cdot)$ can be applied to modify it and the inequality (19) can be further expressed as follows.

$$\begin{aligned} \mathbb{P}(E_1) &\leq \sum_{m'_{\text{wrong}}} \mathbb{P}\left(D(m'_{\text{wrong}}) \leq (1+\varepsilon) \sigma^2 \sum_{i=1}^{n/k} l_i\right) \\ &\leq \sum_{m'_{\text{wrong}}} \min(1, R_1) \\ &= (2^k - 1) 2^{n-k} \min(1, R_1), \end{aligned} \quad (21)$$

where R_1 is calculated by

$$R_1 = \frac{1}{\Gamma\left(1 + \sum_{i=1}^{n/k} l_i / 2\right)} \left(\frac{\pi (1+\varepsilon) \sigma^2 \sum_{i=1}^{n/k} l_i}{2^{2c}} \right)^{\sum_{i=1}^{n/k} l_i / 2}, \quad (22)$$

The union bound of probability can also be further modified by $\min(1, \cdot)$, and then the upper bound of $\mathbb{P}(E_1)$ is

$$\mathbb{P}(E_1) \leq \min\{1, (2^k - 1) 2^{n-k} \cdot \min(1, R_1)\}. \quad (23)$$

It can be done similarly by applying the chernoff bound and the union bound of probability as we do for $\mathbb{P}(E_1)$. It holds that

$$\mathbb{P}(E_2|\bar{E}_1) \leq \min \{1, (2^k - 1) 2^{n-2k} \cdot \min(1, R_2)\}, \quad (24)$$

where

$$R_2 = \frac{1}{\Gamma\left(1 + \frac{\sum_{i=2}^{n/k} l_i}{2}\right)} \left(\frac{\pi (1+\varepsilon) \sigma^2 \sum_{i=2}^{n/k} l_i}{2^{2c}} \right)^{\sum_{i=2}^{n/k} l_i / 2}. \quad (25)$$

Then, by generalizing (23) and (24), we can have

$$\mathbb{P}(E_i|\bar{E}_1, \dots, \bar{E}_{i-1}) = \min \{1, (2^k - 1) 2^{n-ik} \cdot \min(1, R_i)\}. \quad (26)$$

Finally, the FER of Spinal codes, i.e., P_e , can be expressed as follows.

$$\begin{aligned} P_e &= \mathbb{P}(E_1 \cup E_2 \cup \dots \cup E_{n/k}) \\ &= 1 - \prod_{i=1}^{n/k} \mathbb{P}(\bar{E}_1, \dots, \bar{E}_{i-1}). \end{aligned} \quad (27)$$

Let $\epsilon_1 = \mathbb{P}(E_1)$ and $\epsilon_i = \mathbb{P}(E_i|\bar{E}_1, \dots, \bar{E}_{i-1})$, Eq. (27) can be rewritten as

$$P_e \leq 1 - \prod_{i=1}^{n/k} (1 - \epsilon_i). \quad (28)$$

At last, by substituting Eq. (26) into Eq. (28), the proof of Theorem 3 is finished. \square

B. FER Upper Bound of Spinal Codes over BSC

Theorem 4. (New FER upper bound of Spinal codes over BSC) Consider Spinal codes with message length n and segmentation parameter k transmitted over a BSC with crossover probability f . Let l_j be the number of symbols generated from the j^{th} spine value of the n -bit message sequence, then the FER under ML decoding can be upper bounded by

$$P_e \leq 1 - \prod_{i=1}^{n/k} (1 - \epsilon_i), \quad (29)$$

with

$$\epsilon_i = \sum_{a=0}^{N_i} \left(\binom{N_i}{a} f^a (1-f)^{N_i-a} \cdot \min(1, R_{i,a}) \right). \quad (30)$$

Note that

$$R_{i,a} = (2^k - 1) 2^{n-ik} \sum_{t=0}^a \binom{N_i}{t} 2^{-N_i}, \quad (31)$$

where

$$N_i = \sum_{j=i}^{n/k} l_j. \quad (32)$$

The general idea of the proof of Theorem 4 is somehow similar to that of Theorem 3, and thus we provide the detailed proof in Appendix A.

Remark 2. The above derived tight FER upper bounds of Spinal codes in the FBL regime can not only facilitate the

transmission scheme optimization in the next section, but also provide theoretical support and guidance for design of high-efficiency coding-associated techniques, such as unequal error protection and concatenation with outer codes.

IV. TRANSMISSION SCHEME DESIGN

In this section, we aim to optimize the transmission scheme of Spinal codes, using the derived FER upper bounds in Section III. By formulating and solving a code rate maximization problem, we obtain that under ML decoding, the maximum rate can be achieved by incremental tail transmission scheme. While for the practical bubble decoding, as it is difficult to interpret the FER under Bubble decoding algorithm, we design a heuristic improved transmission scheme. The heuristic transmission scheme is inspired by the incremental tail transmission scheme under ML decoding algorithm. Simulations show that the proposed optimized transmission scheme can significantly improve the code rate of Spinal codes with Bubble Decoding.

A. Problem Formulation and Solution

In order to optimize the rate performance of Spinal codes, we establish a rate maximization model under the constraint of sufficiently small FER in this subsection. To formulate the problem, we first emphasize the two related fundamental parameters, i.e., the code rate and the FER, as follows.

- *Code rate:* Consider Spinal codes with message length n and segmentation parameter k transmitted over a channel, let l_j be the number of symbols generated from the j^{th} spine value of the n -bit message sequence, then the code rate can be calculated by

$$R = \frac{n}{\sum_{i=1}^{n/k} l_i}. \quad (33)$$

- *FER:* Based on the theoretical analysis of Spinal codes, for the AWGN channel, the FER can be tightly upper bounded by Theorem 3; for the BSC channel, the FER can be tightly upper bounded by Theorem 4.

For Spinal codes with message length n and segmentation parameter k , the rate maximization problem can be expressed as:

1) Objective function: The maximum code rate R_{\max} , which is denoted by Eq. (33).

2) Constraint: To ensure that the transmitted symbols can meet certain prescribed requirement on successful decoding level; we set

$$P_e^{\text{upper}} = 1 - \prod_{i=1}^{n/k} (1 - \epsilon_i) \leq \delta, \quad (34)$$

where the value of δ can be preset according to specific application requirements.

3) Decision variables: The number of symbols generated from each spine value, $L = \{l_i\}$, $i = 1, 2, \dots, n/k$.

To sum up, the overall optimization problem can be formulated as follows.

Problem 1. For Spinal codes transmitted over the AWGN channel:

$$\begin{aligned} \max R &= \frac{n}{\sum l_j} \\ \text{s.t.} \quad &\begin{cases} P_e^{upper} = 1 - \prod_{i=1}^{n/k} (1 - \varepsilon_i) \leq \delta \\ l_j \in Z^+ \\ \varepsilon_i = \min(1, (2^k - 1) 2^{n-ik} \times \min(1, R_i)) \end{cases} \end{aligned} \quad (35)$$

where R_i is defined in Theorem 3 and Z^+ stands for the positive integer set.

Problem 2. For Spinal codes transmitted over the BSC:

$$\begin{aligned} \max R &= \frac{n}{\sum l_j} \\ \text{s.t.} \quad &\begin{cases} P_e^{upper} = 1 - \prod_{i=1}^{n/k} (1 - \varepsilon_i) \leq \delta \\ l_j \in Z^+ \\ \varepsilon_i = \sum_{a=0}^{N_i} \left(\binom{N_i}{a} f^i (1-f)^{N_i-i} \cdot \min(1, R_{i,a}) \right) \end{cases} \end{aligned} \quad (36)$$

where $R_{i,a}$ and N_i are defined in Theorem 4.

The above problems are nonlinear integer programming problems. To solve a nonlinear integer programming problem, the Branch-Bound algorithm is a general method, however, the iterative mode of the Branch-Bound method requires a large amount of computation and it is likely to converge to a locally optimal solution. Therefore, we design an algorithm customized for the problems above, which can solve the problem globally.

The general idea is to consider the dual problems rather than solving them directly. Taking Problem 1 as an example, its dual problem is as following.

Problem 3. The dual problem of **Problem 1**:

$$\begin{aligned} \min P_e^{upper} &= 1 - \prod_{i=1}^{n/k} (1 - \varepsilon_i) \\ \text{s.t.} \quad &\begin{cases} \sum l_j = N \\ l_j \in Z^+ \end{cases} \end{aligned} \quad (37)$$

In essence, the dual problem above is to determine the decision variables $L = \{l_j\}$ under the constraint of the fixed code rate n/N , so as to minimize the FER of the transmission scheme for certain number of coded symbols, denoted by N . Though the difference between the dual problem and the original problem is just a simple exchange of the constraint and the objective function, the constraint corresponding to the decision variables in the dual problem is a linear constraint, which is much simpler than the original problem.

We devise an on-the-fly algorithm to solve the problem. By ‘on-the-fly’, the minimum FER is found dynamically and iteratively, with increasing number of transmitted symbols. Specifically, only one symbol is considered to be transmitted at a time, and thus the increasing step size of N is 1. At each iteration, the transmitter figures out the current most error-prone symbol to transmit. Once the FER upper bound meets the condition that $P_e^{upper} \leq \delta$, the algorithm is terminated and the decision variables related to the number of transmission symbols are output. Since the FER of Spinal codes decreases

when the number of transmission symbols increases, the number of transmission symbols corresponding to the output of the algorithm is also the minimum one under the constraint of the prescribed small FER δ . Meanwhile, the minimum number of transmission symbols corresponds to the maximum bit rate. Therefore, the original problem of rate maximization under the constraint of a prescribed small FER δ is solved. The details of the algorithm is given in Algorithm 1.

Algorithm 1 The algorithm for solving Problem 1 and Problem 2.

-
- 1: Initialization: $L = [r, r, r, \dots, r, r]$, $N = r \cdot n/k$.
 - 2: Calculate P_e^{upper} by applying Theorem 3 (for problem 1) or Theorem 4 (for problem 2).
 - 3: **while** $P_e^{upper} \geq \delta$ **do**
 - 4: update the number of transmitted symbols: $N \leftarrow N + 1$
 - 5: **for** $i \leftarrow 1$ to n/k **do**
 - 6: update the decision variable: $l_i \leftarrow l_i + 1$
 - 7: calculate and store the corresponding FER $P_{e,i}^{upper}$
 - 8: restore the decision variable: $l_i \leftarrow l_i - 1$
 - 9: **end for**
 - 10: search for the minimum $P_{e,i}^{upper}$ together with the corresponding index d
 - 11: $l_d \leftarrow l_d + 1$
 - 12: **end while**
 - 13: **return** L
 - 14: **end**
-

Remark 3. The value of δ can be preset based on specific application requirements. For example, typical ultra-reliable and low latency communication (URLLC) systems commonly require FER lower than 10^{-5} . In simulations, we set $\delta = 10^{-5}$.

B. Optimal Transmission Scheme with ML Decoding

By solving the problem above, we can obtain the optimal transmission scheme of Spinal codes with the ML decoding algorithm. We begin with a case study, in which we set the message length $n = 32$, the segmentation parameter $k = 4$ and the initial transmission pass $r = 3$. Using Algorithm 1, the results are obtained and shown in Table I.

TABLE I
THE TRANSMISSION SCHEME OVER THE BSC AND AWGN CHANNEL

(a)	
Crossover probability of the BSC	Decision variables
0.05	$L = [3, 3, 3, 3, 3, 3, 3, 30]$
0.01	$L = [3, 3, 3, 3, 3, 3, 3, 25]$
0.005	$L = [3, 3, 3, 3, 3, 3, 3, 22]$
0.001	$L = [3, 3, 3, 3, 3, 3, 3, 20]$
(b)	
SNR (dB) of the AWGN	Decision variables
6	$L = [3, 3, 3, 3, 3, 3, 3, 24]$
7	$L = [3, 3, 3, 3, 3, 3, 3, 19]$
8	$L = [3, 3, 3, 3, 3, 3, 3, 16]$
9	$L = [3, 3, 3, 3, 3, 3, 3, 13]$

It can be seen from Table I that, with ML decoding algorithm, the transmitter tends to continuously transmit the

tail symbols, i.e., the symbols generated from the $(n/k)^{th}$ spine value. This ‘incremental-tail-transmission’-pattern result can be explained and generalized universally by the serial coding structure of Spinal codes. Due to the structure, the conditional error probability $\mathbb{P}(E_i|\overline{E}_1, \dots, \overline{E}_{i-1})$ analyzed in Section III is related to the number of symbols generated after segment m_i , which also means that for Spinal codes, the tail symbol is more relevant to the whole message sequence and hence carries more information. Therefore, the incremental tail transmission scheme is the most efficient transmission scheme under the ML decoding algorithm.

We can also obtain the optimal transmission order of symbols within the same pass by Algorithm 1. In the above case study, if we add an extra constraint that the transmitter takes priority of transmitting a complete pass, by recording the index of the minimum $P_{e,i}^{upper}$ at each iteration, we can obtain the result as $\vec{g} = [8, 7, 6, 5, 4, 3, 2, 1]$. This optimal transmission order can be generalized universally as $\vec{g} = [n/k, n/k - 1, \dots, 2, 1]$, which will be used later in the next subsection.

In summary, the procedures for the optimal transmission scheme with ML decoding are described in Algorithm 2.

Algorithm 2 The incremental tail transmission scheme for ML decoding

- 1: Transmit a complete pass for the decoder to build an integral decoding tree: $j \leftarrow 1$.
 - 2: **while** not receiving an ACK **do**
 - 3: $j \leftarrow j + 1$
 - 4: Transmit the tail symbol $x_{n/k,j}(M)$
 - 5: **end while**
 - 6: end
-

Remark 4. The ML decoding algorithm is difficult to be applied in a practical communication system due to its exponential complexity. Though not applicable, it provides the ideal benchmark performance of Spinal codes. Furthermore, the related analysis and transmission scheme design can serve as an inspirational basis for the transmission scheme design with more practical decoding algorithms.

C. Improved Transmission Scheme with Bubble Decoding

In this subsection, inspired by the incremental tail transmission scheme for ML decoding algorithm, we also propose an improved transmission scheme which combines the uniform puncturing with the incremental tail transmission scheme for the practical bubble decoding algorithm based Spinal codes.

As introduced in Section II. B, the bubble decoding is a kind of asymptotic ML decoding algorithm. It prunes the branch at each layer and retains only B nodes with the lowest cost. It is obvious that the decoding will succeed only if the decoder prunes the branch correctly at every layer of the decoding tree.

Recall that the cost is calculated as

$$Cost = \sum_{i=1}^{layer} \sum_{j=1}^{l_i} \|y_{i,j} - x_{i,j}(M')\|, \quad (38)$$

where *layer* denotes the currently extended number of layers. Since the calculation of the cost at each layer is only related to the preceding received symbols, i.e., $y_{i,j}$ with $i \leq layer$, inadequate transmission of preceding symbols may result in an incorrect pruning, and thus directly leads to a decoding error. Therefore, for the bubble decoding algorithm, merely transmitting the tail symbols without considering the sufficiency of transmission of preceding symbols is not rational. In addition, in the pruning process of bubble algorithm, the previous layer will retain B candidate sequences, while the last layer will retain only 1 candidate sequence, which means that the pruning of the bubble algorithm in the last layer is more prone to errors.

Algorithm 3 The improved transmission scheme for bubble decoding

- 1: Initialization: set the transmission order as $\vec{g} = [n/k, n/k - 1, \dots, 2, 1]$
 - 2: Transmit a complete pass for the decoder to build a integral decoding tree: $j \leftarrow 1, N \leftarrow n/k$.
 - 3: **while** not receiving an ACK **do**
 - 4: $j \leftarrow j + 1$
 - 5: **for** $i \leftarrow 1$ to n/k **do**
 - 6: $N \leftarrow N + 1$
 - 7: **if** $N \leq T_r$ **then**
 - 8: Transmit the coded symbol $x_{g_i,j}(M)$
 - 9: **else**
 - 10: $j \leftarrow j + 1$
 - 11: **break**
 - 12: **end if**
 - 13: **end for**
 - 14: Transmit the tail symbol $x_{n/k,j}(M)$
 - 15: **end while**
 - 16: end
-

Considering the analysis above, we propose the improved transmission scheme for bubble decoding as follows. It combines the uniform puncturing with the incremental tail transmission, forming a two-stage scheme. The first stage adopts the uniform puncturing based transmission, aiming to refine the code rate granularity and more importantly, to ensure the pruning at the preceding levels of the decoding tree is correct. After sufficient symbols have been sent, the transmitter switch to the second stage, which adopts the incremental transmission scheme, aiming to improve the probability that the correct candidate sequence is selected within the B -node list at the last layer. Let T_r denote the switch-over threshold of the number of transmitted symbols, the detailed procedures of the improved transmission scheme for bubble decoding are described in Algorithm 3.

The value of the switch-over threshold T_r in Algorithm 3 can be set according to the following inferences: with the increasing of the number of transmitted symbols N , the instantaneous code rate of the rateless code $R = n/N$ decreases; when the instantaneous code rate approaches the channel capacity C , it is highly probable that the previous pruning is correct. Therefore, we can set $T_r \approx n/C$. In this work, we provide the following heuristic settings, by which

we have obtained satisfactory simulation performance, as will be shown in Section VI.

- For the AWGN channel,

$$T_r = \left\lfloor \frac{n}{C_{AWGN}} - \frac{n}{k} \right\rfloor. \quad (39)$$

- For the BSC,

$$T_r = \left\lfloor \frac{n}{C_{BSC}} \right\rfloor. \quad (40)$$

V. BUBBLE DECODING WITH MEMORY (BD-M)

In essence, both the uniform puncturing and the proposed improved transmission scheme improve the rate performance by refining the code rate granularity of Spinal codes. However, the refinement of code rate granularity increases the number of decoding attempts at the receiver, which results in high time complexity. To solve this problem, we propose the bubble decoding with memory (BD-M) algorithm in this section, which matches well with the proposed improved transmission scheme and reduces the average decoding time without sacrificing rate performance. The combination of the improved transmission scheme at the transmitter and the BD-M algorithm at the receiver constitutes an optimized transmission system, which not only improves the rate performance but also improves the decoding efficiency of Spinal codes.

A. Decoding Process of BD-M Algorithm

The bubble decoding is a full-tree-updating based algorithm, i.e., it needs to repeatedly reconstruct the integral decoding tree once receiving any new sub-passes or symbols. However, for a decoder with memory, we find that it is not necessary to repeatedly reconstruct the complete decoding tree. Instead, the decoder can store the constructed decoding tree in memory and updates only a part of it according to the currently received symbols.

Specifically, according to Eq. (38), the pruning decision of each layer depends only on the received symbols corresponding to this layer and the preceding layers. Therefore, we find observe that the structure of the preceding $i - 1$ layers of the pruned decoding tree could be kept unchanged if the receiver receives a symbol generated by the i^{th} message segment. Based on this observation, we design the BD-M, which is a partial-tree-updating based algorithm.

The main decoding process of the BD-M algorithm can be summarized into four steps:

- 1) Construct a pruned decoding tree according to the received integral pass. The pruning rule inherits from the original bubble decoding algorithm.
- 2) Store the pruned decoding tree.
- 3) If the decoder receives symbol $y_{i,j}$, it will retain the $i - 1$ layers of the previous state of the decoding tree and renew the information after it according to the pruning principle of the bubble decoding algorithm.
- 4) Repeat steps 2) and 3) until the decoding process is finished.

It can be observed that, the proposed BD-M algorithm does not change the Bubble decoding-based pruning decision at

each layer, since the cost of each node calculated by Eq.(38) remains unchanged. The core idea of the BD-M algorithm is to restore the unchanged tree information and reduce the recalculation.

Remark 5. The BD-M algorithm can be applied to both the uniform puncturing based transmission and the proposed improved transmission scheme to reduce the decoding time complexity. Yet it matches better with the proposed improved transmission scheme. As described in Algorithm 3, the improved transmission scheme tends to transmit more tail symbols. Correspondingly, the BD-M algorithm running at the decoder only needs to update the last layer of the decoding tree when receiving tail symbols.

B. Complexity Analysis

During the decoding process, the computation involved at each layer of the decoding tree mainly includes the cost calculating and the bubble sorting for all the nodes at the layer. Let x denote the number of nodes at a certain layer, $f(x)$ represent the associated computation amount.

Firstly, we analyze the number of nodes at each decoding tree layer. According to the decoding process, the branch pruning starts if $2^{ik} \geq B$, where i denotes the layer index of the decoding tree. Thus, we have

$$x_i = \begin{cases} 2^{ik} & 1 \leq i \leq \left\lceil \frac{\log_2 B}{k} \right\rceil \\ B \cdot 2^k & \left\lceil \frac{\log_2 B}{k} \right\rceil < i \leq \frac{n}{k} \end{cases}, \quad (41)$$

where x_i denotes the number of nodes at the i^{th} layer.

Let o_i denote the amount of computation required to update the decoding tree from the i^{th} layer, it can be expressed by

$$o_i = \sum_{j=i}^{n/k} f(x_j). \quad (42)$$

It is obvious that $o_1 > o_2 \dots > o_{n/k}$ and o_1 denotes the computation amount required to reconstruct the full decoding tree.

Next, we analyze the total computation amount required by different transmission-decoding pairs and compare them.

1) *Uniform Puncturing with Bubble Decoding vs. Uniform Puncturing with BD-M:*

For the uniform puncturing with the original bubble decoding algorithm, the decoder needs to reconstruct the full decoding tree when receiving any sub-passes or symbols, so the total computation amount can be expressed as

$$O_{\text{uniform puncturing} \rightarrow \text{bubble decoding}} = \sum_{i=1}^{n/k} l_i o_1. \quad (43)$$

where l_i is the number of transmitted symbols generated from the i^{th} spine value required to successfully recover the message when the uniform puncturing is used.

For the uniform puncturing with the BD-M algorithm, the decoder will not reconstruct the full decoding tree but retain the existing decoding tree in memory and update only a part

of it. The corresponding total computation amount can be expressed as

$$O_{\text{uniform puncturing} \rightarrow \text{BD-M}} = \sum_{i=1}^{n/k} l_i o_i. \quad (44)$$

It is easy to see that Eq. (43) is much larger than Eq. (44) since $o_1 > o_2 \dots > o_{n/k}$, showing that the proposed BD-M requires less computation than the original bubble decoding.

2) *Uniform Puncturing with BD-M vs. Proposed Transmission Scheme with BD-M:*

Let l'_i denote the number of transmitted symbols generated from the i^{th} spine value required to successfully recover the message when using the proposed improved transmission scheme. The total computation amount of the proposed transmission scheme with BD-M can be expressed as

$$O_{\text{the proposed scheme} \rightarrow \text{BD-M}} = \sum_{i=1}^{n/k} l'_i o_i, \quad (45)$$

Compare (44) with (45), we can prove that

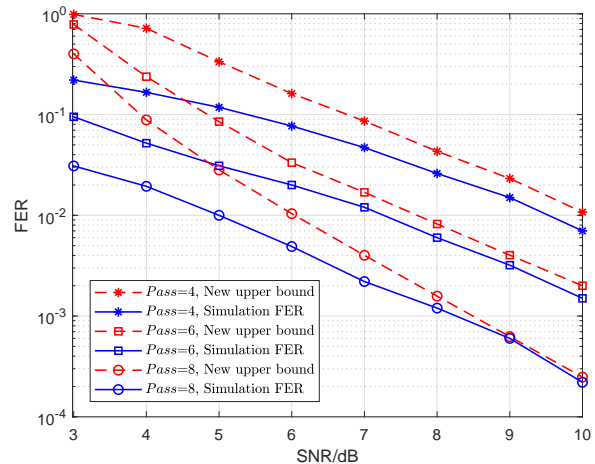
$$\sum_{i=1}^{n/k} l_i o_i \geq \sum_{i=1}^{n/k} l'_i o_i, \quad (46)$$

which demonstrates the superiority of the proposed transmission scheme. As a result, the improved transmission scheme at the transmitter together with the matching BD-M algorithm at the decoder consist of an optimized transmission system for Spinal codes. The proof of (46) is given in Appendix B.

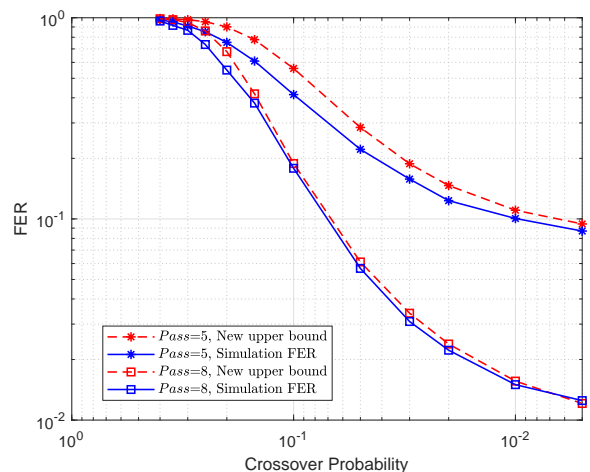
VI. SIMULATION RESULTS

In this section, extensive simulations are conducted to verify the tightness of the FER upper bounds we derive in Section III, to demonstrate the rate performance of the improved transmission scheme we propose in Section IV, and to show the complexity reduction of the BD-M algorithm we propose in Section V.

Fig. 3 shows the comparison of FER performance between the new upper bounds derived in this paper and the simulation results. The simulations are carried out with the ML decoding. To ensure the realizability of the ML decoding algorithm, we set the parameter n as short as 8. We conducted multiple groups of simulations under the conditions of different settings of $Pass$ over the BSC and the AWGN channel respectively to verify the tightness of the derived FER upper bounds, where the parameter $Pass$ denotes the the number of passes the receiver received. According to Fig. 3. (a), for the AWGN channel, the new upper bound fits well with the simulation results when the SNR is high. The large gap at the low SNR regime is mainly due to corresponding looseness of Eq. (20), where the volume of the ball may be bigger than the volume of the cube when the noise variance is large; yet we care more about the moderate-to-high SNR regime, since the corresponding low FER is of more practical value. It can also be observed that the gap generally narrows as the number of passes increases, which can be explained by the property of chernoff bound. Fig. 3. (b) shows that for the BSC, the derived



(a) FER over the AWGN Channel with $c = 8$.



(b) FER over the BSC with $c = 1$.

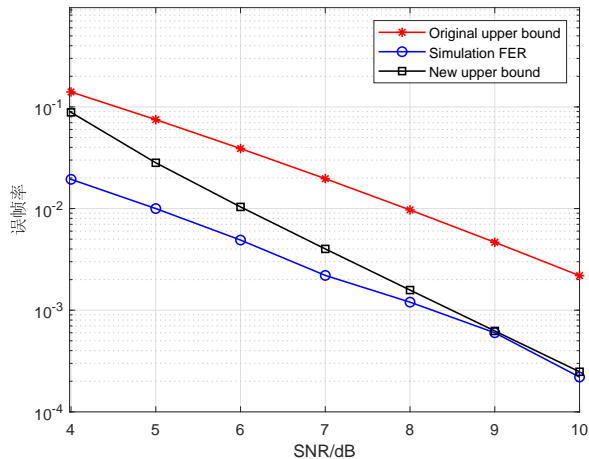
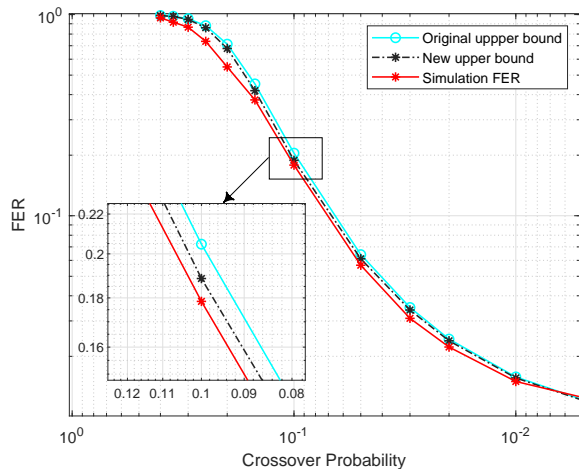
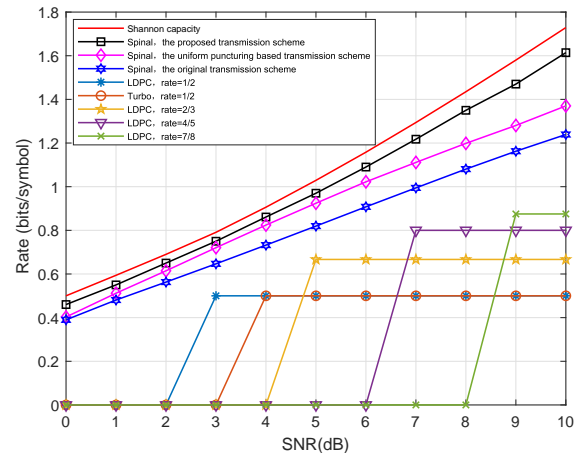
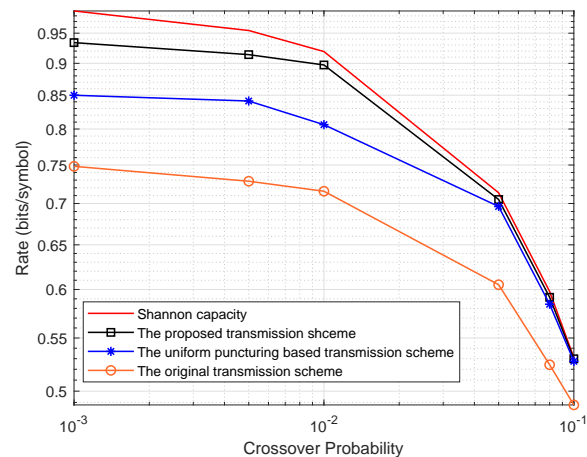
Fig. 3. Comparison between the simulation results and the new tight upper bounds of FER with $n = 8$ and $k = 2$.

FER upper bound is close to the simulation results in a wide range of crossover probability variations.

Fig. 4 gives the comparison between the original FER upper bound proposed in [19] (labeled with ‘Original upper bound’) and the new tight FER upper bound derived in this paper. From Fig. 4. (a), it can be seen that the original upper bound of FER over AWGN shows an overall large gap with the simulation FER, while the new FER upper bound approaches the simulation FER better. In Fig. 4. (b), it is evident that the gap between the original FER upper bound and the simulation curve is very close, however, the new upper bound derived in this paper further narrows the gap and thus provides a more exact FER approximation of Spinal codes over the BSC.

Fig. 5 shows the rate performance comparisons over the AWGN channel and the BSC. It can be seen that the proposed improved transmission scheme outperforms the original pass-by-pass transmission scheme as well as the uniform puncturing based transmission scheme, over both AWGN and BSC.

Fig. 6 gives the average normalized decoding time of different ‘transmission scheme - decoding algorithm’ pairs. It can be

(a) FER over the AWGN channel with $c = 8$.(b) FER over the BSC with $c = 1$.Fig. 4. Comparison between the original upper bounds and the new upper bounds of FER with $n = 8$, $k = 2$ and $P_{\text{ass}} = 8$.(a) Rate performance over the AWGN channel with $c = 8$.(b) Rate performance over the BSC with $c = 1$.Fig. 5. Rate performance Comparison among various channel codes and different transmission schemes with $n = 32$, $k = 4$ and $B = 64$.

seen that the proposed transmission scheme shows lower time complexity than the uniform puncturing based transmission scheme. The reason is that the improved transmission scheme requires fewer number of coded symbols to be transmitted, thus reducing the number of decoding attempts at the decoder. Furthermore, it can be seen from Fig. 6 that the proposed BD-M algorithm reduces the decoding time for not only the uniform puncturing but also the improved transmission scheme, showing its advantage of decoding efficiency over the original bubble decoding. In comparison, the decoding time reduction is more obvious for the improved transmission scheme than for the uniform puncturing, verifying that the BD-M matches better with the improved transmission scheme. In all, the results show that the improved transmission scheme combined with the BD-M algorithm together serve as an optimized transmission system for Spinal codes, which has not only high rate performance but also low decoding time complexity.

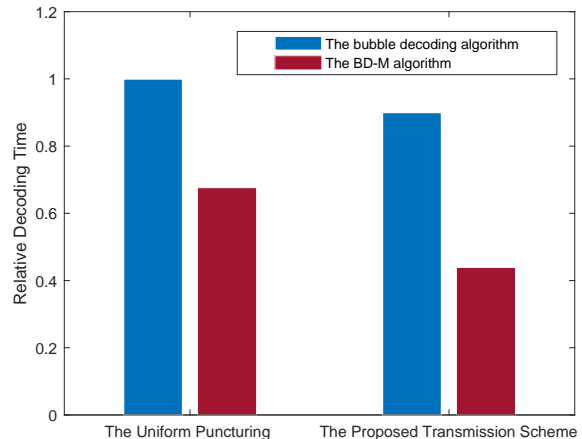


Fig. 6. The average normalized decoding time of different 'transmission scheme - decoding algorithm' pairs.

VII. CONCLUSIONS

In this paper, we have analyzed the error probability of Spinal codes over both the BSC and the AWGN channel, and derived the new tight FER upper bounds. Based on the derived upper bounds, the improved transmission scheme is designed to further increase the code rate of Spinal codes. Furthermore, to solve the problem of large amount of computation in tentative decoding, the BD-M algorithm is proposed in this paper. The work in this paper may also stimulate further research interests and efforts in related topics. The derived tight FER upper bounds can provide theoretical support and guidance for design of high-efficiency coding-associated techniques, such as unequal error protection and concatenation with outer codes. Besides, the general idea of the bubble decoding-based BD-M decoding algorithm may also be used to further improve the decoding efficiency of other decoding algorithms in the literature, such as FSD with memory and BBD with memory.

APPENDIX A PROOF OF THEOREM 4

Given message $M = (m_1, m_2 \dots, m_{n/k})$. Let $x_{i,j}(M)$ denote the j^{th} coding symbols generated from the i^{th} spine value s_i of the n -bit message M and $y_{i,j}$ denote the corresponding symbols received by the receiver. For the ML decoding rules over BSC, the Euclidean distance should be replaced by the Hamming distance as

$$\begin{aligned} \hat{M} &= \arg \min_{M' \in (0,1)^n} \|\mathbf{y} - \mathbf{x}(M')\| \\ &= \arg \min_{M' \in (0,1)^n} \sum_{i=1}^{n/k} \sum_{j=1}^{l_i} \|y_{i,j} \oplus x_{i,j}(M')\|, \end{aligned} \quad (47)$$

where M' denotes the candidate sequence and l_i is the number of symbols generated from the i^{th} spine value of the n -bit message M .

In order to analyze the error probability, the candidate sequence set $(0,1)^n$ are classified into two subsets: one is the unique correct sequence M'_{correct} which satisfies $M'_{\text{correct}} = M$; the other is the wrong sequence, denoted as M'_{wrong} , which is a set including a series of wrong sequences. Since the decision of the ML decoding algorithm is essentially related to the decoding cost of each candidate sequence, we analyze the decoding cost of the candidate sequences in M'_{correct} and M'_{wrong} , respectively.

(1) Firstly, we analyze the cost of the candidate sequence in M'_{correct} , which is denoted by $D(m'_{\text{correct}})$.

$$D(m'_{\text{correct}}) = \sum_{i=1}^{n/k} \sum_{j=1}^{l_i} \|y_{i,j} \oplus x_{i,j}(m'_{\text{correct}})\| \quad (48)$$

Since the crossover probability of BSC is f , it is easy to know that $D(m'_{\text{correct}})$ obeys binomial distribution. As a result, we have

$$\mathbb{P}(D(m'_{\text{correct}}) = a) = \binom{N_1}{a} f^a (1-f)^{N_1-a}, \quad (49)$$

where N_1 is defined in Eq. (32).

(2) Secondly, we analyze the cost of the candidate sequences in M'_{wrong} .

An error will occur only if there exists an $m'_{\text{wrong}} \in M'_{\text{wrong}}$ which satisfies $D(m'_{\text{wrong}}) \leq D(m'_{\text{correct}})$. The FER of Spinal codes can be expressed by

$$P_e = \mathbb{P}(\exists m'_{\text{wrong}} : D(m'_{\text{wrong}}) \leq D(m'_{\text{correct}})). \quad (50)$$

Let $M'_{\text{wrong}} = [m'_1, m'_2 \dots, m'_{n/k}]$ denote the set of wrong sequence with $m'_1 \neq m_1$ and let E_i represent the event that there exists an error in the i^{th} segment, by using the union bound of probability, the probability of E_1 can be bounded as

$$\begin{aligned} \mathbb{P}(E_1) &\leq \sum_{m'_{1\text{wrong}}} \mathbb{P}(D(m'_{1\text{wrong}}) \leq D(m'_{\text{correct}})) \\ &= \sum_{a=0}^{N_1} \mathbb{P}(D(m'_{\text{correct}}) = a) \sum_{m'_{1\text{wrong}}} \mathbb{P}(D(m'_{1\text{wrong}}) \leq a). \end{aligned} \quad (51)$$

According to the idealized hypothesis mentioned in remark 1, it is easy to verify that all the coded symbols $x_{i,j}(M')$ and $x_{i,j}(m'_{1\text{wrong}})$ are independent of each other with Bernoulli distribution. Therefore, it turns out that

$$\mathbb{P}(D(m'_{1\text{wrong}}) \leq a) = \sum_{t=0}^a \binom{N_1}{t} 2^{-N_1}. \quad (52)$$

Thus, by substituting (49) and (52) into (51), we can have

$$\begin{aligned} \mathbb{P}(E_1) &\leq \sum_{a=0}^{N_1} \binom{N_1}{a} f^a (1-f)^{N_1-a} \\ &\quad \min \left(1, |M'_{1\text{wrong}}| \sum_{t=0}^a \binom{N_1}{t} 2^{-N_1} \right) \\ &= \sum_{a=0}^{N_1} \left(\binom{N_1}{a} f^a (1-f)^{N_1-a} \cdot \min(1, R_{1,a}) \right). \end{aligned} \quad (53)$$

where $|M'_{1\text{wrong}}|$ describes the size of set $M'_{1\text{wrong}}$ with $|M'_{1\text{wrong}}| = (2^k - 1) \cdot 2^{n-k}$. Note that

$$R_{1,a} = (2^k - 1) 2^{n-k} \sum_{t=0}^a \binom{N_1}{t} 2^{-N_1}, \quad (54)$$

where

$$N_1 = \sum_{j=1}^{n/k} l_j. \quad (55)$$

Let \bar{E}_i denote the negation of event E_i , and we derive the upper bound of $\mathbb{P}(E_2|\bar{E}_1)$ in the following. For the upper bound of $\mathbb{P}(E_2|\bar{E}_1)$, by similarly applying the union bound of probability, it holds that

$$\begin{aligned} \mathbb{P}(E_2|\bar{E}_1) &\leq \sum_{m'_{2\text{wrong}}} \mathbb{P}(D(m'_{2\text{wrong}}) \leq D(m'_{\text{correct}})) \\ &= \sum_{i=0}^{N_2} \mathbb{P}(D(m'_{\text{correct}}) = i) \sum_{m'_{2\text{wrong}}} \mathbb{P}(D(m'_{2\text{wrong}}) \leq i), \end{aligned} \quad (56)$$

where $m'_{2\text{wrong}} \in M'_{2\text{wrong}}$ and $M'_{2\text{wrong}} = [m'_1, \dots, m'_{n/k}]$ denotes the set of the wrong sequences with $m'_1 = m_1$ and $m'_2 \neq m_2$. Similarly, it is easy to verify that

$$\mathbb{P}(E_2|\bar{E}_1) \leq \sum_{a=0}^{N_2} \left(\binom{N_2}{a} f^a (1-f)^{N_2-a} \cdot \min(1, R_{2,a}) \right). \quad (57)$$

Then, by generalizing (53) and (57), we can have

$$\mathbb{P}(E_i|\bar{E}_1, \dots, \bar{E}_{i-1}) \leq \sum_{a=0}^{N_i} \left(\binom{N_i}{a} f^a (1-f)^{N_i-a} \cdot \min(1, R_{i,a}) \right). \quad (58)$$

At last, by substituting (58) into (28), the proof of Theorem 3 is finished.

APPENDIX B PROOF OF (46)

For the improved transmission scheme which combines the uniform puncturing with the incremental tail transmission, it is easy to find that

$$l'_1 \leq l_1, l'_2 \leq l_2, \dots, l'_{n/k-1} \leq l_{n/k-1}, l'_{n/k} \geq l_{n/k} \quad (59)$$

Besides, as the rate corresponding to the improved transmission scheme is higher than the rate when using the uniform puncturing, it turns out that

$$\sum_{i=1}^{n/k} l_i \geq \sum_{i=1}^{n/k} l'_i. \quad (60)$$

According to (59), we assume that $l'_i + r_i = l_i$ for $1 \leq i \leq n/k - 1$ and $l'_{n/k} - r_{n/k} = l_{n/k}$, where $r_i \geq 0$. Substituting them into (60), we can have

$$\sum_{i=1}^{n/k-1} r_i \geq r_{n/k}. \quad (61)$$

Therefore, we obtain that

$$\begin{aligned} \sum_{i=1}^{n/k} (l_i - l'_i) o_i &= \sum_{i=1}^{n/k-1} r_i o_i - r_{n/k} o_{n/k} \\ &\geq \sum_{i=1}^{n/k-1} r_i o_i - \sum_{i=1}^{n/k-1} r_i o_{n/k} \\ &= \sum_{i=1}^{n/k-1} r_i (o_i - o_{n/k}) > 0. \end{aligned} \quad (62)$$

REFERENCES

- [1] J. Xu, S. Wu, J. Jiao and Q. Zhang, "Optimized Puncturing for the Spinal Codes," *2019 IEEE International Conference on Communications (ICC)*, Shanghai, China, pp. 1-5, 2019.
- [2] A. Li, S. Wu, Y. Wang, J. Jiao and Q. Zhang, "Spinal Codes over BSC: Error Probability Analysis and the Puncturing Design," *2020 IEEE 91st Vehicular Technology Conference (VTC2020-Spring)*, Antwerp, Belgium, pp. 1-5, 2020.
- [3] J. Perry, H. Balakrishnan, and D. Shah, "Rateless spinal codes," in *Proc. ACM HotNets*, Art. no. 6, 2011.
- [4] H. Balakrishnan, P. Iannucci, J. Perry, and D. Shah, "De-randomizing shannon: The design and analysis of a capacity-achieving rateless code," *CoRR*, vol. abs/1206.0418, 2012.

- [5] J. Ha, J. Kim, and S. W. McLaughlin, "Rate-compatible puncturing of low-density parity-check codes," *IEEE Transactions on Information Theory*, vol. 50, no. 11, pp. 2824-2836, 2004.
- [6] S. Sesia, G. Caire, and G. Vivier, "Incremental redundancy hybrid ARQ schemes based on low-density parity-check codes," *IEEE Transactions on Communications*, vol. 52, no. 8, pp. 1311-1321, 2004.
- [7] R. Karp, M. Luby, and A. Shokrollahi, "Finite length analysis of LT codes," *International Symposium on Information Theory*, p. 39, 2005.
- [8] A. Shokrollahi, "Raptor codes," *IEEE Transactions on Information Theory*, vol. 52, no. 6, pp. 2551-2567, 2006.
- [9] U. Erez, M.D. Trott, and G. W. Wornell, "Rateless coding for Gaussian channels," *IEEE Transactions on Information Theory*, vol. 58, no. 2, pp. 530-547, 2012.
- [10] F. Jelinek, "Fast sequential decoding algorithm using a stack," *Ibm Journal of Research and Development*, vol. 13, no. 6, pp. 675-685, 2010.
- [11] S. Xu, S. Wu, J. Luo, J. Jiao and Q. Zhang, "Low Complexity Decoding for Spinal Codes: Sliding Feedback Decoding," *2017 IEEE 86th Vehicular Technology Conference (VTC-Fall)*, Toronto, ON, pp. 1-5, 2017.
- [12] Y. Hu, R. Liu, H. Bian and D. Lyu, "Design and Analysis of a Low-Complexity Decoding Algorithm for Spinal Codes," *IEEE Transactions on Vehicular Technology*, vol. 68, no. 5, pp. 4667-4679, 2019.
- [13] J. Hagenauer, "Rate-compatible punctured convolutional codes (RCPC codes) and their applications," *IEEE Trans. Commun.*, vol. 36, no. 4, pp. 389-400, Apr. 1988.
- [14] D. G. M. Mitchell, M. Lentmaier, A. E. Pusane and D. J. Costello, "Randomly Punctured LDPC Codes," *IEEE Journal on Selected Areas in Communications*, vol. 34, no. 2, pp. 408-421, Feb. 2016.
- [15] R. Wang and R. Liu, "A Novel Puncturing Scheme for Polar Codes," *IEEE Communications Letters*, vol. 18, no. 12, pp. 2081-2084, Dec. 2014.
- [16] J. Perry, P. A. Iannucci, K. E. Fleming, H. Balakrishnan, and D. Shah, "Spinal codes," *ACM Sigcomm Computer Communication Review*, vol. 42, no. 4, pp. 49-60, 2012.
- [17] Y. Li, J. Wu, B. Tan, M. Wang and W. Zhang, "Compressive Spinal Codes," *IEEE Transactions on Vehicular Technology*, vol. 68, no. 12, pp. 11944-11954, 2019.
- [18] R. G. Gallager, *Information theory and reliable communication*, 1968.
- [19] X. Yu, Y. Li, W. Yang, and Y. Sun, "Design and Analysis of Unequal Error Protection Rateless Spinal Codes," *IEEE Transactions on Communications*, vol. 64, no. 11, pp. 4461-4473, 2016.
- [20] H. Balakrishnan, P. Iannucci, J. Perry, and D. Shah, "De-randomizing shannon: The design and analysis of a capacity-achieving rateless code," *Mathematics*, 2012.
- [21] Y. Polyanskiy, H. V. Poor, and S. Verdú, "Channel coding rate in the finite blocklength regime," *IEEE Transactions on Information Theory*, vol. 56, no. 5, pp. 2307-2359, 2010.